THE SPONGE-LIKE TOPOLOGY OF LARGE-SCALE STRUCTURE IN THE UNIVERSE

J. Richard Gott III
Department of Astrophysical Sciences, Princeton University

Adrian L. Melott[1]
Astronomy and Astrophysics Center and Enrico Fermi Institute, University of Chicago

AND

Mark Dickinson
Department of Astrophysical Sciences, Princeton University
Received 1985 August 12; accepted 1986 January 3

ABSTRACT

An important problem in cosmology is characterizing the topology of the large-scale structure in the universe. There has been a debate between hierarchical clustering models in which clusters are high-density islands in a low-density sea, and cell structure models in which voids are isolated low-density islands in a high-density sea. To examine the relative connectedness of the high- and low-density regions we have constructed maps with a density contour chosen so that the high- and low-density regions occupy equal volumes. We find that the CfA catalog shows a sponge-like topology. The high- and low-density regions are both connected. They are equivalent and completely interlocking. The boundary surface between the high- and low-density regions has an average negative curvature and is characterized by a large number of holes. Such a result is plausible theoretically because the initial conditions in both cold dark matter scenarios and massive neutrino scenarios have sponge-like topologies. The high- and low-density regions in the initial conditions must be equivalent because they are due to random quantum fluctuations, and a change in sign would reverse their roles. The topology does not change at all as long as the fluctuations are in the linear regime, and on the scales of interest the fluctuations are only just now coming out of the linear regime. In the cold dark matter and neutrino scenarios the typical hole sizes are of order the smoothing diameter or the damping length, whichever is larger. The sponge-like topology explains how the universe can have a rather frothy appearance without being organized into regular cells. A computer algorithm for measuring topology is proposed.

Subject headings: cosmology — galaxies: clustering

I. INTRODUCTION

One of the important problems in cosmology today is characterizing the nature of the topology of the large-scale structure in the universe. There have been two major competing models: the hierarchical clustering model (Soniera and Peebles 1978) and the cell structure of the universe model (Joeveer and Einasto 1978). The present paper proposes a third alternative, namely that the large-scale structure of the universe exhibits a sponge-like topology.

Clusters and superclusers have been known for some time. The richest of these have total luminosities of several hundred L_* ($L_* \approx 8.5 \times 10^9 h^{-2}$ $L_\odot$, where $h = H_0/100$ km s^{-1} Mpc^{-1}) and represent density enhancements of at least a factor of several over the background. The existence of these objects naturally leads to the hierarchical clustering picture in which clusters are seen as islands of high density in a low-density sea. In fact, Soniera and Peebles (1978) have produced simulations of the observed clustering by starting with an empty space and placing spherical clusters at random within it. Within each cluster, subclusters are placed in a hierarchical sequence. This kind of model appears natural in a cold dark matter model (see Peebles 1982; Blumenthal et al. 1984) where galaxies form first and then cluster gravitationally. This is a model in which the high-density regions are seen as isolated clumps, while the low-density regions constitute a single connected region. This model is like white polka-dots on a black background.

The cell structure model of Joeever and Einasto is based on the adiabatic fluctuation model of Doroskevich, Sunyaev, and Zeldovich (1974), who found that if the fluctuations on small scales are damped (as occurs with baryonic adiabatic models and massive neutrino models), caustics will form causing material to collide on sheets or pancakes. The sheets then fragment into galaxies. In this model the superclusters are the pancakes and form before the galaxies. Joeever and Einasto characterized the final state as cells filling space (like a honeycomb), with the interiors of the cells being essentially empty and the cell walls being the high-density regions. The cells form a space-filling tesselation of polyhedrons. Galaxies reside in the walls. Where three or more walls meet at an edge, gravity will cause more galaxies to congregate there, forming a denser filament. Where four or more edges meet at a vertex, a dense cluster will form (see Matsuda and Shima 1983). Filaments and walls seen edge on are supposed to be responsible for the filamentary appearance of the Shane and Wirtanen counts and other samples. This picture is one in which isolated voids (the cell interiors) exist in one connected high-density medium, like black polka dots on a white background. Topologically the cell structure model (which is like a honeycomb) is identical to a "Swiss cheese" model in which one starts with a uniform high-density medium and excises "tremas" or voids from it. In fact, Mandelbrot (1983) has produced a simulation of galaxy clustering by starting with a uniform high-density distribution of galaxies and then excising randomly placed spherical volumes. Adding to the validity of this model is the

[1] Enrico Fermi Postdoctoral Fellow.

fact that large voids do in fact exist, perhaps the most famous being the Bootes void discovered by Kirshner *et al.* (1981). This is a region at least 6000 km s$^{-1} = 60h^{-1}$ Mpc in diameter ($h = H_0/100$ km s^{-1} Mpc^{-1}) in which no bright galaxies have been found so far. The region must be at least several times less dense than the average. If filled to average density, this void would have contained a total luminosity of $L \approx 1700\, L_*$. There are no Abell clusters in this void, but there are some near its edges, consistent with the cell picture (Bahcall and Soniera 1983). It is interesting that the amount of luminosity missing from the largest voids is comparable to the amount of luminosity contained in the largest superclusters (see Aarseth, Gott, and Turner 1979).

Shandarin (1982) developed a test designed to discriminate between these two models. He centers a bubble of radius r on each galaxy. If r is small enough, the bubbles will be isolated, but for some critical value of r_{crit} the bubbles will percolate, and it will be possible to walk across the entire sample region (in this case he studies a region of size $40h^{-1}$ Mpc) going only through chains of linked bubbles. Let r_p be the value of r_{crit} for percolation for a Poisson distribution of galaxies. For the hierarchical picture we expect that $r_{crit} > r_p$ because the bubbles will have to be larger to get us from one isolated cluster to another. For the cell structure model we expect $r_{crit} < r_p$ because high-density regions are already connected, and in fact simulations with adiabatic fluctuations with a lower damping cutoff, as in the Zeldovich pancake picture, do show this. Shandarin finds that the real sky shows $r_{crit} < r_p$ so that the high-density regions do appear to be connected, and the cell structure model is favored. On the other hand, Melott *et al.* (1983) and Davis *et al.* (1985) found that cold dark matter (CDM) scenarios also have $r_{crit} < r_p$, even though galaxy clusters do grow in a hierarchical fashion in these models, presumably as a result of the large amount of power on large scales.

At the IAU conference on large-scale structure in Crete, Einasto and Miller (1983) showed three-dimensional views of galaxy distributions based on all available redshifts assembled by J. Huchra. This was presented in a movie in which the distribution of galaxies was rotated so that one could see a three-dimensional effect. The visual impression was not in good agreement with either of the simple hierarchical or cell structure scenarios. There were some clusters and some voids, but the sky was messier than either model. Clusters appeared to be connected to each other in a lazy, haphazard fashion, but voids did not appear to be isolated in cells. Instead, they seemed to spill sloppily into each other in a random fashion. The distribution did have a somewhat frothy character, as expected from the cell structure picture, but one did not actually see cells enclosing voids. Thus neither model appeared to give an accurate representation of the topology of the data.

Historically it is interesting to note that a similar problem of topology occurred in the study of solar granulation. Here the object was to determine whether the solar granules represented just some form of general random turbulence or were really organized into convection cells. What was done (Schwarzschild, private communication) was to obtain a high-quality photograph at the best possible resolution and make a high-contrast print such that half the surface area of the photograph was white and half was black. If the granules were really organized into convection cells, the hot rising cell interiors should be white on the photograph, and the cool cell walls should be black. Thus the photograph should look like white polka dots on a black background. This was in fact the case, confirming the existence of convection cells.

We will do the same thing in three dimensions with the galaxy distribution. Since galaxies are discrete points (δ-functions in density), we first will smooth the data. This can always be done in principle by convolving the data with a Gaussian smoothing function whose width is at least of order the mean galaxy-galaxy separation: $\sigma \sim (\bar{n})^{-1/3}$, where $\bar{n}$ is the mean number density of galaxies brighter than some cutoff, say $L \approx 0.85L_*$. Then we will have a smooth function of density as a function of position in three dimensions. Now separate the sample into high- and low-density regions, where the dividing line is chosen so that the total volume occupied by the high- and low-density regions is exactly equal. The high-density regions are thus defined as regions where the density is higher than the median value.

What does the picture look like? Is it white polka dots on a black background, or black polka dots on a white background? We are so conditioned to looking at two-dimensional pictures that it is easy to come to the erroneous conclusion that if the high-density regions are connected, the low-density regions must not be, and vice versa. In fact, as we shall see in the next section a third possibility exists in three dimensions: that the high- and low-density regions are both connected and interlocking in a sponge-like topology.

II. TOPOLOGY OF THE HIGH- AND LOW-DENSITY REGIONS

For our observational sample we will use the CfA catalog with complete redshifts down to magnitude 14.5. For our purposes we want a volume-limited cubical sample. We will put the Earth at one vertex of the cube. From our location this cubical volume will subtend one octant of the celestial sphere. We want to pick an octant of the sky that will be included in the Zwicky catalog ($\delta > 0°$) and which is at high galactic latitude. We pick the octant defined by the spherical triangle ABC, where A is at $\delta = 90°$, B is at $\delta = 0°$, $\alpha = 9^h49^m$, C is at $\delta = 0°$, $\alpha = 15^h49^m$ (1950). The triangle is centered on the north galactic pole in right ascension and lies entirely in the Zwicky catalog. The vast majority of the triangle lies at galactic latitude $b_{II} > 40°$. The only part that is below $b_{II} = 40°$ is a small triangular region $13°$ across near vertex A and two really negligible triangular regions $\sim 1°$ across near vertices B and C. Since galactic apsorption is low and perhaps negligible above $b_{II} = 40°$, we will not make any absorption corrections. This should be quite satisfactory over most of the cube, but we will keep in mind that we may miss some galaxies in the small region near vertex A. Below $b_{II} = 40°$ we can miss galaxies due to absorption and to the fact that the CfA catalog is not guaranteed to be complete below this galactic latitude. Next we need to pick the size of the cube. We wish to pick the largest cube, in which the number of galaxies in the volume-limited sample is still near the maximum. If the cube is picked too small it will include many faint galaxies, but its volume will be so small that the total number of galaxies is also small. If the cube is too big, the absolute magnitude cutoff required will be such that only a few galaxies make it. We have adopted a cube with a diagonal length of $50h^{-1}$ Mpc and a side length of $L = 28.9h^{-1}$ Mpc. (A similar volume-limited sample in a cube with a $40h^{-1}$ Mpc side would have had less than half as many galaxies, for example.) From the CfA catalog down to 14.5 mag we construct a volume-limited sample including all galaxies brighter than $M_B = -18.99 + 5 \log h$ ($= 0.72L_*$). Galaxies are placed at their redshift distances in the usual way after the Earth's motion of $V = 300$ km s^{-1} in the direction $l_{II} = 90°$, $b_{II} = 0°$ has been subtracted. The sample includes 153 galaxies and includes the Virgo supercluster and beyond, reaching

almost to the Coma cluster which lies just beyond the cube's diagonal from the Earth. The number of galaxies present is sufficient to construct a good number density in a $4 \times 4 \times 4$ array of 64 cells, each $7.2h^{-1}$ Mpc on a side. The mean number of galaxies per cell is 2.39. The median density is one galaxy per cell. Twenty-seven of the 64 cells have zero galaxies; 26 cells have two or more galaxies. Thus, most of the low-density cells have no galaxies in them at all, while most of the high-density cells have two or more. Since peculiar velocities of galaxies are generally less than 700 km s^{-1}, these cells are sufficiently large so that peculiar velocities will not typically cause galaxies to be erroneously placed in cells. One clear exception to this is the Virgo cluster core where peculiar velocities have clearly smeared the cluster over two adjacent cells. But this is of no real consequence for us since both of those cells would be above the median in any case. The density is assumed constant within each cell and then is smoothed with a cubical hatbox smoothing function of total width $l = 6.3h^{-1}$ Mpc $= 7L/32$ (just a bit smaller than one cell). (Smoothing an initial data set with a cubical hatbox smoothing function of total width l means that the density at a particular point in the smoothed data set is equal to the average density in a cubical volume l^3 centered on that point in the unsmoothed initial data set.) This produces a smooth density distribution throughout the cube where the effective total smoothing length is approximately $\lambda_c \approx 9.6h^{-1}$ Mpc. This is evaluated on a $32 \times 32 \times 32$ grid. To eliminate boundary effects periodic boundary conditions are adopted, a choice which facilitates later comparisons with large N-body fast Fourier simulations where this is used. The median density is determined by starting at a high-density contour where only a small fraction of the $32 \times 32 \times 32$ grid points are above it and lowering it by increments of 2% until at least half the grid points are above it. Because of the clustering the median density ρ_m in the smoothed sample is significantly below the mean: $\rho_m = 0.73\bar{\rho}$. Setting the contour level at the median number density we then construct pictures of the high

and the low-density regions in Figure 1. Figure 1a shows the high-density regions. The Earth is at the bottom front vertex, and the north celestial pole is in the vertical direction. The Virgo cluster is just above the bottom face near the center. Figure 1b shows the low-density regions.

Several comments can be made about this picture. First of all, the high-density parts form one connected region; i.e., it is possible to travel from any point in the high-density region to any other without ever leaving it. (Recall that because of the periodic boundary conditions, when one exits the top of the cube one reenters the cube at the bottom; similarly with the front and back and left and right faces.) Second, the low-density parts also form one connected region. Mathematically this is known as a sponge (Mandelbrot 1983). The body of a marine sponge forms one connected region; the sea water also forms one connected region percolating throughout the sponge. Another way of saying this is to note that there is only one supercluster and only one void. Sponges are characterized by many holes; chambers are connected by tunnels. Thus both the high- and low-density regions are multiply connected. This means we can make a number of complete cuts in the high- (or low-) density region before it falls apart into two pieces. The region has a high genus number. (We will discuss this property further in the next section). The high- and low-density regions are completely interlocking. Remarkably, the high- and low-density regions are geometrically quite equivalent and indistinguishable from each other. This sponge-like topology fits in well with the quantitative picture one gets looking at Einasto and Miller's (1983) three-dimensional galaxy calalog. The high-density regions are connected and do percolate, just as Shandarin found. However, the low-density regions also percolate so that voids flow into each other rather than being surrounded on all sides by high-density regions.

We note at this point that there is a low-density region along the nearest vertical edge of the cube near the top. This is the most distant part of the cube near $\delta = 90°$ and is the only part
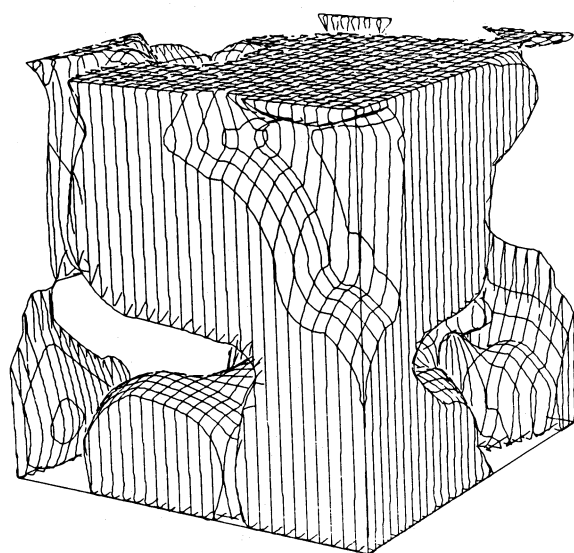
CfA-HIGH DENSITY

Fig. 1a
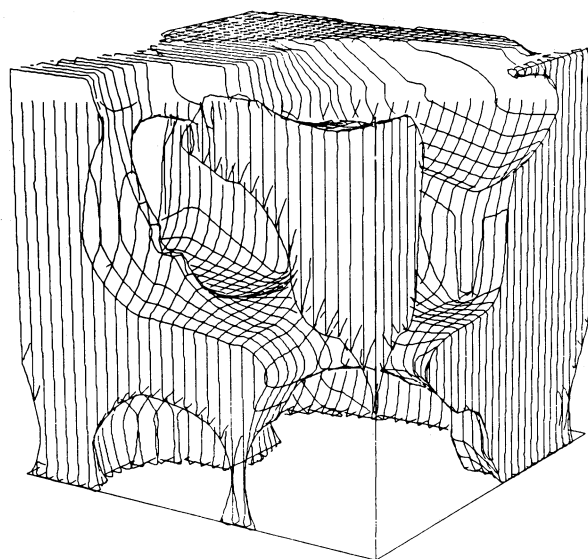
CfA-LOW DENSITY

Fig. 1b

Fig. 1.—CfA volume limited sample. Earth is at the bottom front corner. Cube side length is $28.9h^{-1}$ Mpc. (a) High-density region; (b) low density region. Periodic boundary conditions assumed in Figs. 1–6, 9, 12, 13.

of the cube likely to have been affected by galactic obscuration and completeness. Note that if this were changed to a high-density region it would not affect any of the conclusions above.

Not only are the high- and low-density regions both connected, and both percolate, but they are completely interlocked. The high- and low-density regions are completely equivalent. Looking just at figures 1*a* and 1*b*, there is really no clue as to which is the high-density one and which is the low-density one. Space has been divided into two interlocking and completely equivalent regions.

Are there any theoretical reasons for the universe showing this sponge-like structure? Interestingly there are. According to inflationary scenarios the fluctuations which lead to galaxies and clusters are due to quantum fluctuations with a Zeldovich power spectrum. At any given scale such fluctuations will have a Gaussian distribution with random phases and as many positive fluctuations as negative fluctuations. If such fluctuations grow by gravitational instability, the growth rate is independent of the amplitude of the fluctuations so the fluctuations retain their Gaussian nature as they grow as long as they stay in the linear regime. Likewise when fluctuations are damped by either Silk damping (for baryons) or Landau damping (for neutrinos), positive and negative fluctuations are damped equally. The end result of this is that if we examine the initial conditions present at recombination where everything is still in the linear regime, we will find that they are exactly symmetric with respect to positive and negative density fluctuations. The high-density regions (where the density is above average) must have the same topology as the low-density regions (below average) because a simple change in sign of the original (totally random) quantum fluctuations would have reversed their roles. Thus at recombination the high-density regions cannot look like white polka dots on a black background. A simple change of sign of the initial quantum fluctuations would turn this into black polka dots on a white background, and the high-density regions would go from being not connected to being connected. The high- and low-density regions must have exactly the same degree of connectedness because their roles are interchangeable. As we have seen, a sponge-like topology allows both the high- and low-density regions to be connected. Furthermore, we can construct sponges whose insides and outsides are identical interlocked regions. As we shall see in the next section, a study of the boundary surface between the high- and low-density regions shows that the surface is expected in general to be negatively curved in order that both sides of the surface be equivalent. This in turn allows us to deduce the fact that the high- and low-density regions should be interlocked with many holes and columns.

We have constructed a map of the high- and low-density regions in the initial conditions $(1 + z = 100)$ of a heavy neutrino model with $\Omega_v = 1$ a Zeldovich $n = 1$ spectrum at large scales and a co-moving Landau damping cutoff scale of $\lambda_c \sim 13(\Omega_v h^2)^{-1}$ Mpc. The cube depicted has a comoving side length of $L = 36 \ (\Omega_v h^2)^{-1}$ Mpc at the present epoch. Since the Landau damping cutoff is not infinitely sharp, choosing an exact value of λ_c is somewhat a matter of convention. We have adopted that of Szalay and Bond (1983), $\lambda_c \approx 41 m_{30}^{-1}$ Mpc $\approx 13(\Omega_v h^2)^{-1}$ Mpc, where m_{30} is the mass of the heaviest neutrino in units of 30 eV and we are assuming that this neutrino is much more massive than the others (see Melott 1983). The model is computed on a grid of $32 \times 32 \times 32$ unit cubes with no smoothing. The boundary conditions are taken to be periodic. Since the perturbations are still in the linear regime,

the median density is equal to the average density. The result is shown in Figures 2*a* and 2*b*. It indeed has a sponge-like topology. The size of the holes and columns in the sponge is approximately equal to $\lambda_c = 0.36L$. There is no structure on scales smaller than this because it has been damped by Landau damping. As expected, the high- and low-density regions are entirely equivalent.

Thus the universe is expected to start off with a sponge-like topology for its high- and low-density regions. How does this change as the universe expands? For a long time after recombination the topology does not change at all. This is because the fluctuations are all in the linear regime and all grow at the same rate $(\delta\rho/\rho) \propto a$, so that the map of density fluctuations in comoving coordinates has exactly the same shape but the amplitudes are all increased. The contour for $\rho = \bar{\rho}$ has an amplitude of $(\delta\rho/\rho) = 0$ and does not move at all as the fluctuations grow. After the fluctuations enter the nonlinear regime, high- and low-density perturbations do have different growth rates and the map can change topology. However, it is important to note that on the scale of galaxy clusters and superclusters we are just barely coming out of the linear regime at the present epoch. In the CfA data the smallest scale we examined was $\lambda \approx 7.2h^{-1}$ Mpc. The observed covariance function is given by $\xi(r) = (r/r_0)^{-1.8}$ for $r < r_0 = 5h^{-1}$ Mpc and $\xi(r) < 1$ for $r > r_0 = 5h^{-1}$ Mpc (see Peebles 1980). Thus the average density fluctuations on scales larger than $7.2h^{-1}$ Mpc are less than one even today. The situation is even somewhat better than this since $\xi(r)$ measures the average density fluctuations, and we are interested in median values. The average value is due in part to occasional fluctuations that are greater than unity. The median values of the density fluctuations are then less than the average. The clustering pattern we are observing is therefore just coming out of the linear regime on the scales of interest, and the topology on large scales should look approximately the same as it did at recombination.

To test this we have run a fast Fourier simulation of this heavy neutrino model using a $32 \times 32 \times 32$ grid with periodic boundary conditions. It is evolved from the initial epoch at $1 + z = 100$ to the present where the initial fluctuation amplitude has been adjusted so that the amplitude of clustering is correct at the present epoch. Figures 3*a* and 3*b* show the high- and low-density regions at the present epoch. The data are computed on a $32 \times 32 \times 32$ grid smoothed with a cubical hat box function of width $7L/32$ just like that used for the CfA data. The boundary is drawn at the median density as measured in the unit cubes of size $L/32$. Because of the nonlinear clustering $\rho_m = 0.64\bar{\rho}$, an effect similar to that seen in the CfA data. The high-density region in both cases is chosen to occupy exactly half the volume. The high-density region at the present epoch also has a sponge-like topology with holes and columns of size λ_c. Comparing Figures 3 and 2, there is a striking similarity. The majority of the holes and columns are in exactly the same positions. The nonlinear effects have caused some changes, occasionally a hole connecting two parts of the low-density regions disappearing, for example.

While there are some differences, the overall agreement is striking. If we want to see a map of the initial conditions of the universe, the CfA map in Figure 1 is about as good as we can do. As an additional experiment we also did a larger massive neutrino simulation with $\lambda_c = 13(\Omega h^2)^{-1}$ Mpc as before, but with $L = 72(\Omega h^2)^{-1}$ Mpc. Again the holes had sizes of order λ_c, but there were many more holes than in Figures 2 and 3 simply because we were examining a larger volume. It also had a
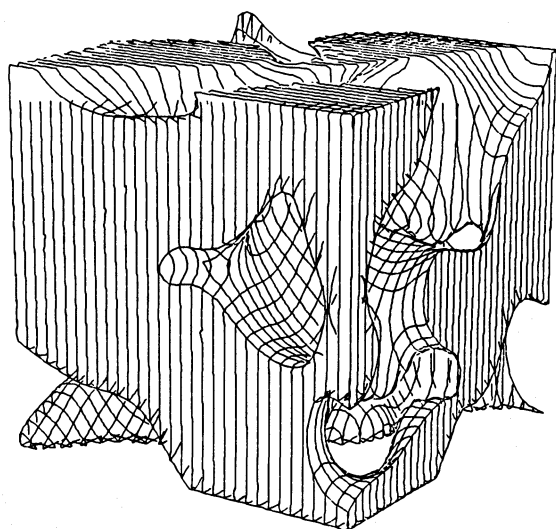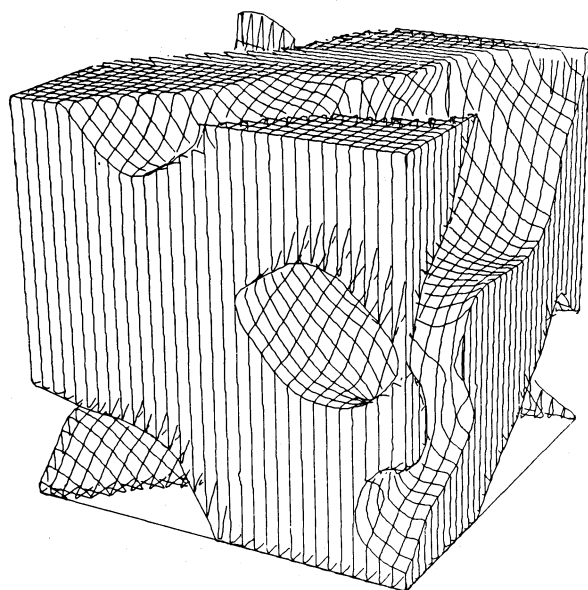
ν-INITIAL

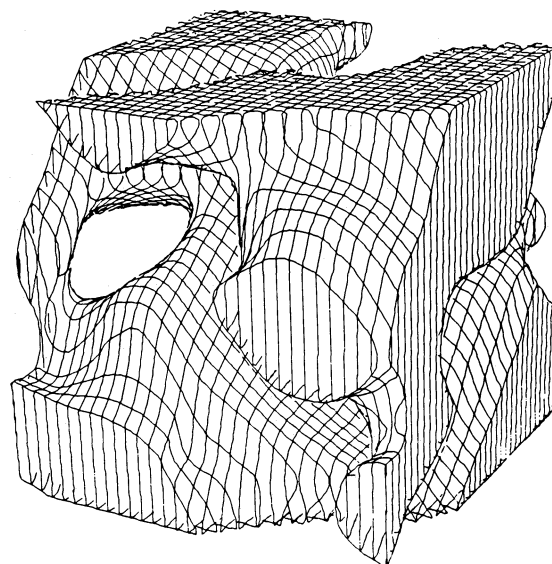HIGH DENSITY

Fig. 2a
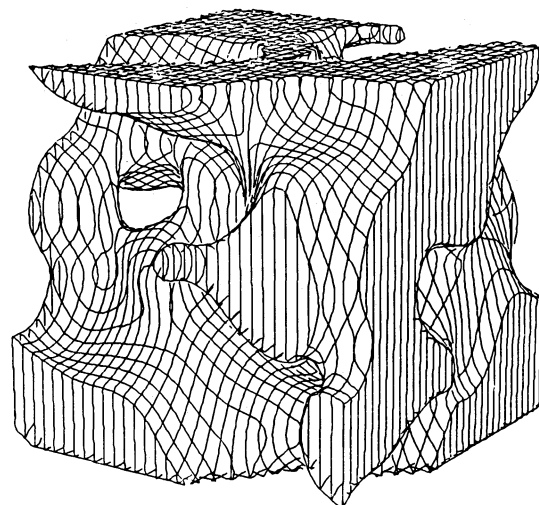
ν-INITIAL

LOW DENSITY

Fig. 2b

Fig. 2.—Initial conditions at $1 + z = 100$ for an $\Omega = 1$ massive neutrino model where the short-wavelength cutoff length is 0.36 of the cube side length which is 36 $(\Omega h^2)^{-1}(1 + z)^{-1}$ Mpc. (a) High-density region; (b) low-density region.

ν-FINAL

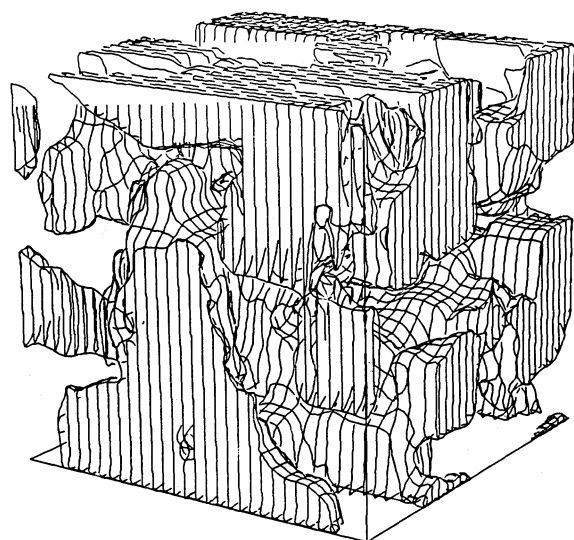HIGH DENSITY

Fig. 3a

ν-FINAL

LOW DENSITY

Fig. 3b

Fig. 3.—Evolution of the $\Omega = 1$ massive neutrino model whose initial conditions are shown in Fig. 2. This figure shows the final conditions at the present epoch. Cube side length is $36(\Omega h^2)^{-1}$ Mpc. (a) High-density region; (b) low-density region.

sponge-like topology, behaving in every way like the simulation in Figures 2 and 3.

An important point to mention here is that the neutrino models do in fact show a sponge-like topology rather than the cell structure topology proposed by Joeveer and Einasto.

Models with cold dark matter (CDM) also show a sponge-like topology where the size of the smallest holes is λ_c, the smoothing length which is adopted. An example of this is shown in Figure 4. This is a CDM model with a primordial inflationary Zeldovich spectrum, a spectrum whose index n

CDM, $\Omega = 1$

FINAL HIGH DENSITY

Fig. 4a
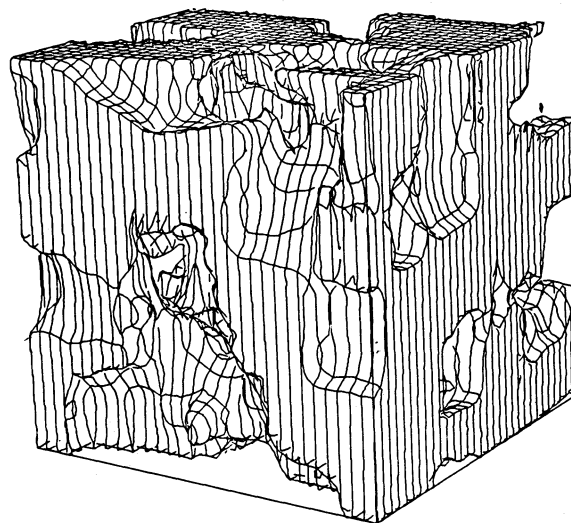
CDM, $\Omega = 1$

FINAL LOW DENSITY

Fig. 4b

Fig. 4.—Cold dark matter, $\Omega = 1$ model final conditions. Cube side length is $36(\Omega h^2)^{-1}$ Mpc. (a) High-density region, (b) low-density region.

goes smoothly from $n = -3$ as small scales to $n = +1$ at large scales $[(\delta\rho/\rho) \propto M^{-(1/2+n/6)}]$. The characteristic scale at which the change in index occurs is the horizon scale when the universe first becomes matter dominated. This is proportional to $(\Omega h^2)^{-1}$. At large scales where $n > 0$ this causes anti-correlations in the covariance function. The covariance function goes negative at a radius $r_c = 18(\Omega h^2)^{-1}$ Mpc, where r is evaluated at the present epoch (Davis *et al.* 1985). This is the type of spectrum which is generally produced in inflationary cosmologies. Gott (1982) and Gott and Statler (1984) have proposed inflationary models with $\Omega < 1$. In these models our universe is produced from a single bubble of asymmetric vacuum. The universe inherits its overall negative curvature from the bubble formation event, and on top of this there is a spectrum of quantum fluctuations which, on the scales of interest, is a primordial Zeldovich spectrum as described above, but with an appropriately low value of Ωh^2. Bahcall and Soneira (1983) have found that Abell clusters have a positive cluster-cluster covariance function out to a radius of $r = 100h^{-1}$ Mpc. If this is to be explained in a CDM model, $\Omega h < 0.18$ (Davis *et al.* 1985). The model shown is a CDM spectrum with $\Omega = 1$ started at $1 + z = 100$ and evolved to the present epoch. The data are computed on a $32 \times 32 \times 32$ grid. Figures 4a and 4b show the results at the present epoch. The cube side length is $L = 36(\Omega h^2)^{-1}$ Mpc. The densities at the present epoch are computed on the $32 \times 32 \times 32$ grid and then smoothed with a cubical hatbox function of total width $\lambda_c = 7L/32 = 7.9$ $(\Omega h^2)^{-1}$ Mpc. The median density is $\rho_m = 0.87\bar{\rho}$. As in previous cases the median is below the mean due to the clustering. The figure shows that the CDM scenario produces a sponge-like topology. The smallest holes and tunnels visible have a size of order λ_c. Some of these tunnels and chambers are longer than λ_c, the size of the largest features perhaps being related to the scale at which the spectrum index n becomes positive: $r_c = 18(\Omega h^2)^{-1}$ Mpc $= \frac{1}{2}L$. This is thus a sponge which may show

two characteristic scales, λ_c and r_c. Further studies on this would be interesting.

In Figure 5 is shown an Aarseth, Gott, and Turner (1979) 4000 body simulation with Poisson initial conditions, a power-law spectrum with $n = 0$. This is similar to the spectral index shown at these scales by CDM inflationary models in which n goes smoothly from -3 to 1, being approximately $n = 0$ on the scale $r_c = 18(\Omega h^2)^{-1}$ Mpc. The model has $\Omega = 0.095$ starts at a redshift of $1 + z = 22.63$ and by the present epoch has a reasonable clustering amplitude. The starting redshift represents the point where the galaxies become density enhancements of order unity and start to gravitate like point masses. These are softened masses with a softening length of $\epsilon \sim 25h^{-1}$ kpc, and they have a Schecter luminosity function. The simulation at the present epoch encompasses a spherical volume $50h^{-1}$ Mpc in diameter. From this we construct a cubical volume-limited sample of $L = 28.9h^{-1}$ Mpc just like the CfA data. Densities are computed on a $4 \times 4 \times 4$ grid and are smoothed just as in the CfA data. Because of the clustering, $\bar{\rho}_m = 0.87\rho$. The result is shown in Figures 5a and 5b. A second model, exactly the same except that it had $\Omega = 1$ and started at $1 + z = 10.73$, was also computed. This model at the present epoch had $\bar{\rho}_m = 0.63\rho$. Both the $\Omega = 1$ and $\Omega = 0.095$ models show a sponge-like topology with hole size approximately equal to the smoothing radius λ_c. These both look quite similar to the CfA data.

As an additional experiment we also did smoothed, pure, power laws with $n = -3$, and $n = +3$. All showed a sponge-like topology.

All the comments about the symmetry of the initial conditions, the fact that the topology remains unchanged throughout the linear regime and that we are just coming out of the linear regime on these scales, apply to the CDM models just as they do to the neutrino models. By doing the smoothing we are effectively building in a short-wavelength cutoff in the spec-
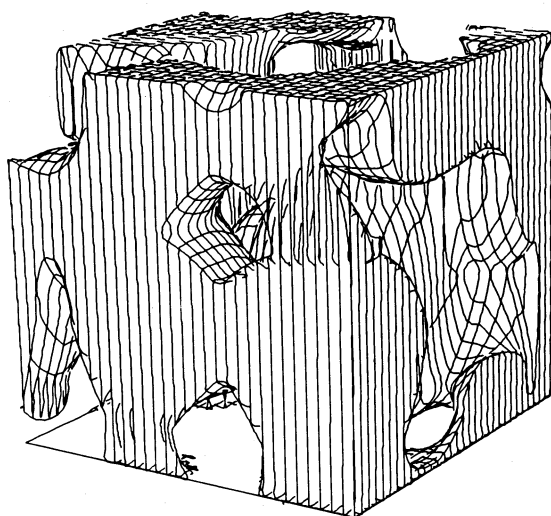
POISSON, $\Omega = 0.095$

FINAL HIGH DENSITY

FIG. 5a
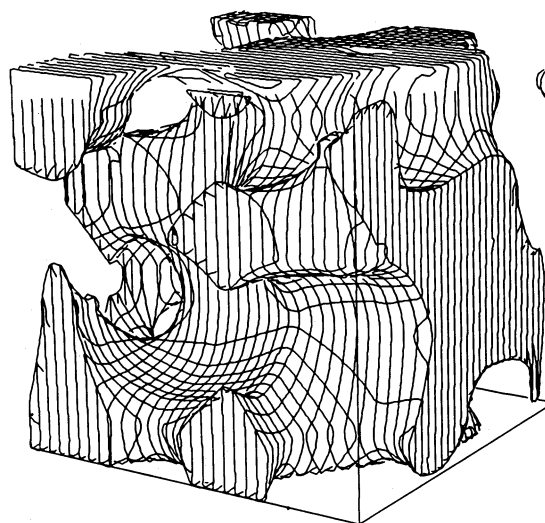
POISSON, $\Omega = 0.095$

FINAL LOW DENSITY

FIG. 5b

FIG. 5.—Poisson, $\Omega = 0.095$ model final conditions. Cube side length is $28.9h^{-1}$ Mpc. (a) High-density region, (b) low-density region.

trum just as that which occurs by damping in the neutrino models. It is interesting to note that the CDM models also produce a sponge-like topology instead of the island cluster topology one might have at first expected.

In principle, one can distinguish between the neutrino and CDM models by counting how the number of holes change as one varies the smoothing length. This will be treated at length in a later paper (Hamilton, Gott, and Weinberg 1986). Roughly speaking, in the CDM model the number of holes per unit volume is $\sim 1/8\lambda_c^3$, where λ_c is the smoothing length we have adopted for the data (see discussion in § III). But in the neutrino model the number of holes per unit volume is $\sim 1/8\lambda_v^3$ only if the adopted smoothing length $\lambda_c > \lambda_v$ (where $\lambda_v = 13[\Omega_v h^2]^{-1}$ Mpc is the Landau damping cutoff scale). If $\lambda_c < \lambda_v$, the number of holes per unit volume remains $\sim 1/8\lambda_v^3$ for all values of adopted smoothing length $\lambda_c < \lambda_v$. Thus if we keep lowering the smoothing length in the neutrino model, the number of holes remains constant beyond a certain point, but in the CDM model the number of holes keeps going up as the smoothing length is lowered. This test is workable as long as the expected neutrino Landau damping scale $\lambda_v = 13 (\Omega_v h^2)^{-1}$ Mpc is larger than the correlation length $r_0 \approx 5h^{-1}$ Mpc. (We always want to pick a smoothing length for the data λ_c larger than the correlation length so that we are looking at fluctuations which are still just coming out of the linear regime; (see Hamilton, Gott, Weinberg 1986 for more details on this.)

Next let us examine the topology produced in a completely different galaxy formation scenario, the explosive blast wave model of Ostriker and Cowie (1981) and Ikeichi (1981). In this picture small seeds trigger galaxy formation in a self-propagating blast wave. This leads to expanding thin spherical shells of recently formed galaxies with voids inside and unprocessed material on the outside. Before percolation occurs, the topology is like the Swiss cheese model, and after percolation occurs it looks like the Joeveer and Einasto cell structure model. In either case the low-density regions are iso-

lated, and the high-density regions are connected. Since this is a nonlinear mechanism, the symmetry arguments about high- and low-density regions do not apply. The most likely scenario is that percolation has in fact occurred. In this case voids should be surrounded on all sides by sheets of galaxies. The problem is what happens to the galaxies once they have formed on these sheets. By gravitational instability they should flow toward the edges of the polyhedral cells. This process can tear holes in the sheets, allowing adjacent voids to be connected and changing the topology to a sponge-like topology.

To test this we have used an Aarseth, Gott, and Turner (1979) simulation with 1000 equal point masses $\Omega = 0.3$ and $(1 + z)_{start} = 5.17$, which is taken to be the redshift at which the galaxies form on the sheets. The simulation has a spherical volume with comoving diameter of $50h^{-1}$ Mpc. Initially the galaxies are placed in Poisson fashion on six planes $X = \pm 8.33h^{-1}$ Mpc, $Y = \pm 8.33h^{-1}$ Mpc, $Z = \pm 8.33h^{-1}$ Mpc (comoving coordinates). This simulates a cell structure based on a regular space filling lattice of cubes of size $16.66h^{-1}$ Mpc. This structure has been suggested by Heavens (1985) as representative of a cell structure type of model. The galaxies are started with a cold Hubble flow and allowed to cluster. As expected, eight large clusters form at the vertices since there is a flow from the faces to the edges and then vertices. Gott and Dickinson (1986) have found that the final conditions of this model have an excellent power-law covariance function with $\xi(r) \propto r^{-2}$. The map of the final conditions is shown in Figures $6a$ and $6b$ with $\rho_m = 0.80\bar{\rho}$. The cube is of size $L = 20h^{-1}$ Mpc, centered on $X = Y = Z = 0$ and parallel with those axes. The data are sampled on a $4 \times 4 \times 4$ grid with smoothing applied just as in the CFA data. Roughly speaking, the high-density regions are the eight corner cells and the 24 edge cells, while the low-density regions are the eight center cells and the 24 face cells. The topology is sponge-like. Is this due to nonlinear tearing of holes in the cell walls or just a result of poor resolution in sampling? It is important to note that we really
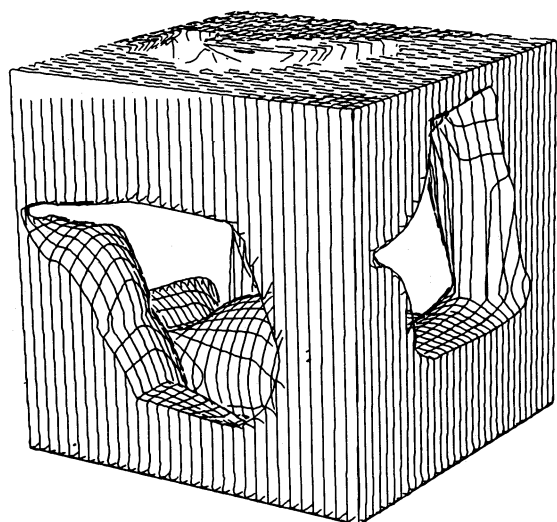
CELL STRUCTURE

FINAL HIGH DENSITY

FIG. 6a
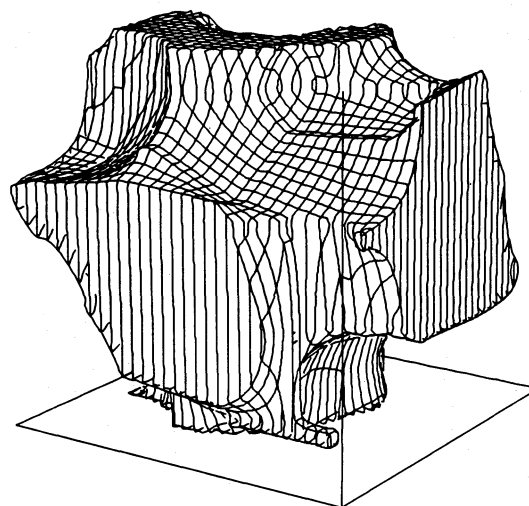
CELL STRUCTURE

FINAL LOW DENSITY

FIG. 6b

FIG. 6.—Final conditions of a model with an initial cell structure geometry. Cube side length is $20h^{-1}$ Mpc. (*a*) High-density region; (*b*) low-density region.

do not have enough resolution in this diagram to study the topology properly. A grid of $16 \times 16 \times 16$ is really required to show the topology of the initial conditions of this model properly. In that case 2744 of the 4096 cells must be empty, the median contours are contained in the void regions, and the voids are correctly shown to be isolated. If the resolution is too poor as in the $4 \times 4 \times 4$ case, then the cell walls appear thicker than they actually are and take up more than half of the volume, and some holes must be punched through them by the median contour at their lowest density points even in the initial conditions. Since we only have 1000 galaxies in our spherical volume, we do not have good enough statistics to do a study at $16 \times 16 \times 16$ resolution. One needs an average of at least two galaxies per unit cell to construct a reasonable median density contour.

This illustrates some of the problems in dealing with realistic data sets which include only bright galaxies. For the present we can note the amount of movement that takes place from the faces to the edges and vertices. Using the $4 \times 4 \times 4 = 64$ unit cells for the cubical volume, in the initial conditions we have an average of 11.5 galaxies per corner cell, 7.6 galaxies per edge cell, 3.8 galaxies per face cell, and zero galaxies per center cell. This distribution simply depends on how many sheets cross through a cell (three perpendicular sheets pass through each corner cell, for example). In the final conditions clusters form approximately in the eight corners. The corner cells have an average of 17.1 galaxies in each. The edge cells have an average of 5.7 galaxies in each, the face cells have an average of 1.1 galaxies in each, and the center cells have an average of zero galaxies in each. Thus there is a significant movement away from the face cells, and the holes through the faces shown in figures 6*a* and 6*b* are quite justified. A study of this at a resolution of $8 \times 8 \times 8$ shows 59% of the face cells to be empty, also leading to holes in the faces. Thus the nonlinear effects of gravitational instability can cause holes to form in the

faces of the cells and convert the topology to a sponge-like topology as well. When holes form in the faces in a cell structure model so that the galaxies are primarily located in the edges of the polyhedral cells, this is usually referred to as a net (see Shandarin and Zeldovich 1983) or a lattice (connected lattice of strings) (Einasto, Klypin, and Shandarin 1983; Einasto *et al.* 1984). A net or a lattice of strings has a sponge-like topology.

In this case it is interesting to note that although the topology is sponge-like it is not necessary that the inside and outside of the sponge be equivalent as is the case for the CDM and neutrino models. With enough resolution we might notice that the high-density regions are thinner, i.e., the probability of a high-density unit cell having a low-density cell as a neighbor would be greater than the probability of a low-density cell having a high-density cell as a neighbor. In the CDM and neutrino models these probabilities would be equal.

Finally we will consider the type of topology which might result from string assisted galaxy formation (Zeldovich 1980; Vilenkin 1981*a*). Note that if strings are sufficiently massive ($\mu = 10^{24}$ g cm^{-1}) to promote galaxy formation, they should also eventually be observable via gravitational lensing (Vilenkin 1981*b*; Gott 1985; Kaiser and Stebbins 1984) and gravitational radiation (Hogan and Rees 1984). Schramm (1985) has noted that if galaxies were preferentially located on or near strings this would naturally produce a $\xi(r) \propto r^{-2}$ covariance function on large scales with no anticorrelations at very large scales, as would be the case in the CDM and neutrino models where $n \rightarrow 1$ as the scale becomes larger than the comoving horizon scale at which the universe becomes matter dominated. Schramm has argued that this, in principle, would make it easier to understand the Bahcall and Soniera result that the Abell clusters have a positive covariance function out to scales of more than $100h^{-1}$ Mpc. (This could be explained in a CDM scenario only if $\Omega h < 0.18$ [Davis *et al.* 1985], but of

course there are low Ω inflationary models available; see Gott 1982; Gott and Statler 1984.) While it is far from clear how and where galaxies would be formed in a realistic string scenario where closed loops of string as well as infinite strings and their motions would have to be considered, we can at least mention what topology would result if galaxies clustered with a topology similar to that of the strings themselves. The high-density regions would be like strands of spaghetti, and the low-density regions would be one connected region. If closed loops were present, there would be some "Spaghetti-O.s" as well. Note that both the high-density and low-density regions would percolate. Shandarin's percolation test would be satisfied because you could construct a string of bubbles that would cross the entire region staying on one high-density strand of spaghetti. This is not a sponge-like topology, however, because the high-density regions are not all connected, they are in separate disconnected strands. The fluctuations associated with string assisted galaxy formation are not Gaussian with random phases, so our arguments about the equivalence of the high- and low-density regions do not apply. One possibility, however, is that galaxy formation would be triggered primarily by small loops which would themselves be reasonably randomly distributed, so that the end result would be to mimic the Poisson case of Figure 5 which would produce a sponge-like topology.

Thus at face value the CfA data are consistent with either the CDM or massive neutrino models and might be consistent with the Ostriker-Cowie model. The holes in the CfA data are about the size of the adopted smoothing length $\lambda_c \approx 9.6 h^{-1}$ Mpc. In the Ostriker-Cowie model the hole size is of order one-half the cell structure size, so the cells should be smaller than $\sim 19 h^{-1}$ Mpc. Hogan (1984) and Vishniac and Ostriker (1985) have pointed out that in the simplest explosion model the maximum cell size must be less than 9 Mpc in order to avoid making fluctuations in the microwave background that are too large. If the bubbles are smaller than 9 Mpc, we could be seeing just the Poisson fluctuations on large scales provided by the small-scale bubbles. For the neutrino model the hole size is expected to be of order the larger of the smoothing length and the Landau damping cutoff $\lambda_c \sim 41 m_{\nu 30}^{-1}$ Mpc, where $m_{\nu 30}$ is the mass of the heaviest neutrino in units of 30 eV. Thus $m_\nu > 130 h$ eV, $\Omega h > 1.35$ (see Doroshkevich et al. 1980; Centrella and Melott 1983; Frenk, White, and Davis 1983; Klypin and Shandarin 1983). As Frenk, White, and Davis (1983) have discussed, there are difficulties in such a model making galaxies early enough to explain quasars. The problem is that the clustering is best explained if we are just coming out of the linear regime now. For galaxies and QSOs to form, we need something to come out of the linear regime before $1 + z \approx 4$. Melott (1985) has noted that this condition may be fulfilled if only a small fraction of the material goes out of the linear regime, since QSOs are rare bright objects. Still, we are at the limits of making such models work. As Frenk, White, and Davis have noted, one way out is if $\Omega_\nu \approx 0.3$, so that superclusters form at $1 + z \sim 4$ but clustering stops growing at $1 + z \sim 3$; hence we are still not much out of the linear regime today. Such an alternative is not available if we need a small value of λ_c. A caveat to mention here is that the CfA sample may not be large enough to constitute a fair sample of the universe. It is possible that we are still looking inside a large-scale high-density region and seeing mass fluctuations in that. Note in this regard that if $\lambda_c \approx 60 h^{-1}$ Mpc is characterized by the structure seen in the Kirschner et al. (1981) void, we have

$\Omega h \approx 0.3$. In our CfA cubical volume the total luminosity in galaxies brighter than $0.72 L_*$ is $L_B = 242 L_*$. With a Schechter luminosity function with index $\alpha \sim 1$, as appears appropriate for the local supercluster (Turner and Gott 1976), then the total luminosity density in the cube including all the faint galaxies below the cutoff is $\sim 1.8 \times 10^8 h\ L_\odot\ \mathrm{Mpc}^{-3}$. This compares with the mean luminosity density for the universe as a whole of $2 \times 10^8 h\ L_\odot\ \mathrm{Mpc}^{-3}$ deduced by Kirshner, Oemler, and Schechter (1979) from a sample out to $r = 200 h^{-1}$ Mpc. This supports the claim that the CfA sample constitutes a fair sample. But in any case we must be somewhat conservative in deducing the value of λ_c for the neutrino model from the CfA data. The CDM scenarios automatically predict hole sizes of order the smoothing length and are therefore in excellent agreement with the data.

In summary, the CfA data show a sponge-like topology. Theoretically, we would expect both CDM and massive neutrino models to show a sponge-like topology. The Ostriker-Cowie explosive galaxy formation scenario would form a cell structure topology, but nonlinear gravitational instability effects could tear holes in the walls and convert it to a sponge-like topology as well. Galaxy formation induced by strings might possibly lead to a spaghetti-type topology.

III. THE BOUNDARY BETWEEN THE HIGH- AND LOW-DENSITY REGIONS

In a sponge-like topology the boundary between the high- and low-density regions is a two-dimensional surface that is multiply connected (has holes like a doughnut) and has an overall average Gaussian curvature which is negative. We will show in this section how these two properties are related. Finally, we will show how the boundary surface may be approximated by a polygon network and how this can lead to a computer algorithm to measure the topology.

The Gaussian curvature of a two-dimensional surface at a particular location is the reciprocal of the product of the two principal radii of curvature at that point:

$$K = \frac{1}{a_1 a_2}. \qquad (1)$$

In a positively curved surface (like a sphere) both radii of curvature point in the same direction and therefore have the same sign. (For a sphere of radius r_0, $K = r_0^{-2}$.) If one of the radii of curvature is infinite, as occurs in a cylinder, then $K = 0$, and indeed a cylinder is intrinsically flat because we can make one out of a flat sheet of paper without tearing or crimping it. Saddle-shaped surfaces are negatively curved because in one direction the surface curves upward and in the perpendicular direction the surface curves downward, giving a_1 and a_2 opposite signs.

For the sponges we are talking about, the boundary surface divides space up into two equal and completely equivalent parts. For a positively curved surface the inside is different from the outside. The enclosed side is in the direction that both radii of curvature point. On the other hand, for a western saddle, both the horse's and rider's sides are equivalent. So a negatively curved boundary surface has the possibility of dividing space into two completely equivalent parts. The basic reason that the sponge boundary is negatively curved is that for such a surface one radius of curvature points into the high-density region while the other radius of curvature points into the low-density side, so that both are on an exactly equal footing.

The Gauss-Bonnet theorem states that for a compact two-dimensional surface the integral of the Gaussian curvature over the surface is given by

$$I = \int K dA = 4\pi(1 - g) , \qquad (2)$$

where g is the genus of the surface. Informally speaking, g is the number of holes the surface has; strictly speaking, it may be defined as the number of closed curves that may be drawn on the surface without cutting it into two separate pieces. The genus of the sphere is 0, the genus of a doughnut is 1. The genus of a sphere with N handles is N. By extension we could say that the genus of two spheres is -1 because they are already separated into two pieces. Note that I is dimensionless because K has units of $(\text{length})^{-2}$, while dA has units of $(\text{length})^2$. By inspection the formula is correct for a sphere where $K = r_0^{-2}$, $A = 4\pi r_0^2$, and $g = 0$. For a torus or doughnut $I = 0$. The inner regions of the torus around the hole are negatively curved, while the regions near the circumference are positively curved.

Any curved surface may be approximated by a network of polygonal faces. A sphere, for example, may be approximated by a polyhedron such as a cube. When such polygon networks are used to approximate a compact surface of genus g, we find that

$$I = \sum D_i = 4\pi(1 - g) , \qquad (3)$$

where $D_i = 360° - \sum V_i$ is the angle deficit at each vertex and V_i are the vertex angles around the vertex. In a plane we expect the sum of the vertex angles of the polygon faces meeting at a vertex to be $360° = 2\pi$. For example, in a checkerboard four squares are around a vertex. Each square has a vertex angle of $90°$ and $4 \times 90° = 360°$, so the angle deficit is zero. But in a cube which approximates a compact surface of genus 0, there are only three squares around a vertex, so $D_i = 360° - 3 \times 90° = 90°$ at each of the eight vertices, giving $\sum D_i = 720° = 4\pi$, as expected. An isocahedron has 12 vertices with five triangles around each vertex. The angle deficit at each vertex is $D_i = 360° - 5 \times 60° = 60°$ and $\sum D_i = 720° = 4\pi$, as expected. What is happening here is that the curvature is being compressed into δ-functions at the vertices. The faces have zero curvature, and so do the edges which are just bent like cylinders. Parallel transport arguments show that the integral of the δ-function of Gaussian curvature over the infinitesimal area of the vertex is just equal to the angle deficit at the vertex. Figure 7 shows another example. We can make a polygon network of 32 squares which approximates a torus. It has eight squares on top, eight squares on the bottom, 12 squares forming the circumference, and four squares forming the hole. There are 32 vertices in the figure: 16 of these vertices have four squares
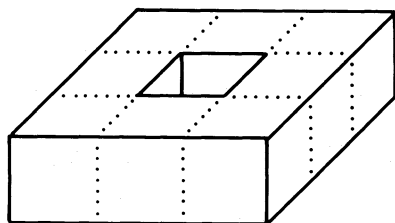
around them and therefore an angle deficit of zero; the eight outer corner vertices have three squares around them and therefore an angle deficit of $90°$ each; the eight inner corner vertices have five squares around them and therefore an angle deficit of $D_i = 360° - 5 \times 90° = -90°$ each. Note that the geometry around the inner vertices is saddle-shaped, with the negative curvature indicated by the negative angle deficit at the vertex. The sum of all the angle deficits for this figure is $I = \sum D_i = 0$ as expected for a surface with $g = 1$. We can construct a surface with two holes out of squares as well. Most vertices will be surrounded by four squares and have zero angle deficit, but there will be eight outer corner vertices with $D_i = +90°$ and one set of eight inner vertices with $D_i = -90°$ for each hole. The total of angle deficits will be $\sum D_i = -720° = -4\pi$, as expected for a surface with $g = 2$.

A regular polygon network in a three-dimensional Euclidean space may be defined as one which is composed of regular polygons, where the disposition of polygons around each vertex is identical. There are five regular polygon networks with positive curvature. They are the five regular polyhedra: tetrahedron (triangles, three around a point), octahedron (triangles, four around a point), isocahedron (triangles, five around a point), cube (squares, three around a point), dodecahedron (pentagons, three around a point). These are all surfaces of genus $g = 0$ with $\sum D_i = 4\pi$. There are three planar networks: checkerboard (squares, four around a point), chicken wire net (hexagons, three around a point), and triangle tesselation (triangles, six around a point). These networks all have $D_i = 0$ and approximate surfaces of zero curvature. Note that in addition to planar configurations these nets can be constructed to approximate cylinders. (Cut four rows out of an infinite checkerboard and bend them around so that the top and bottom edge meet. One has then constructed an infinite tube with square cross section approximating a cylinder. It is regular because each vertex is identical.) Then there are regular polygon networks that are negatively curved. The first of these (squares, six around a point) was discovered by Petrie in 1926 (see Coxeter 1937). Coxeter (1937) discovered two more (hexagons, four around a point, and hexagons, six around a point). Gott (1967) discovered four more (pentagons, five around a point, squares, five around a point, triangles, eight around a point, triangles, 10 around a point). Wells (1969, 1977) discovered three more (triangles, seven around a point, triangles, 9 around a point, triangles, 12 around a point). There are several structural forms for some of these. These are known variously as regular skew polyhedra or pseudopolyhedra, or 3D polyhedra. Some of these are illustrated in Figure 8. It can be seen immediately that these are infinite repeating networks that have a lot of holes and are multiply connected. In all cases they are boundaries of sponges and divide space into two infinite interlocking regions. In some of these cases the two regions are identical to each other, so that the skew polyhedra forms the boundary of a sponge of exactly the kind we are looking for. In the figure, the skew polyhedra (triangles, 10 around a point, squares, six around a point, hexagons, four around a point, pentagons, five around a point, and hexagons, six around a point) divide space into two equivalent regions. One can also construct networks with squares, (five around a point) and triangles (eight around a point), which divide space into two equivalent parts.

Since we will often wish to divide space into cubic lattices for sampling galaxy data, the network (squares, six around a point) is particularly relevant. Imagine a space-filling tessela-

TOROIDAL POLYGON NETWORK

FIG. 7.—Surface of a torus may be approximated by a polygon network

Triangles, 8
around a point.

Triangles, 10
around a point.

Squares, 5 around
a point.

Squares, 6
around a point.

Pentagons, 5
around a point.

Hexagons, 4
around a point.
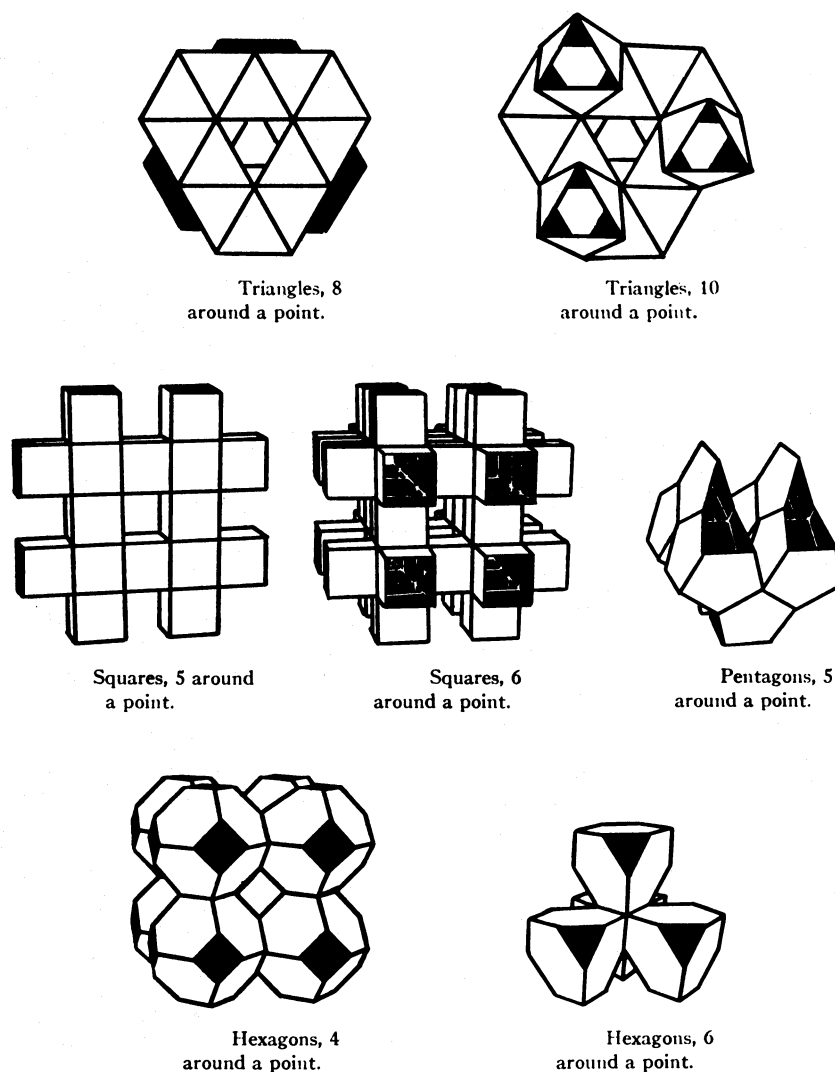
Hexagons, 6
around a point.

Fig. 8.—Boundaries of sponges may be approximated by skew polyhedra: polygon networks with negative curvature (from Gott 1967)

tion of cubes where each has side of length λ_c. We can produce a division of the cubes into high-density and low-density cubes such that the boundary is the configuration squares, six around a point (see Fig. 9). The smallest repeating unit cell for this configuration is one $2 \times 2 \times 2$ cubes. For any repeating surface we can define the genus of the surface per repeat volume as

$$g_s = \frac{-1}{4\pi} \int K \, dA = -\frac{I}{4\pi} \, . \tag{4}$$

The reason for this is that we could always build a finite section of the repeating structure and close off the ends with positively curved sections (vertices with angle deficits) to make a compact surface which obeys the relation $g = -I/4\pi + 1$. In the limit as we make the finite section larger and larger the angle deficits produced by closing off the ends can be ignored because they go up as the square of the size of the region, while the value of the angle deficits from the interior of the region goes up as the cube of the size; the constant term becomes negligible as well. Now there are as many vertices as cubes, and the angle deficit at each is $-180°$ in the squares (six around a point) configu-

ration. So the average angle deficit encountered per cube is $I = -\pi$, and the volume density of holes is

$$\frac{dg_s}{dV} = \frac{1}{4\lambda_c^3} \, . \tag{5}$$

Thus the unit cell which has a volume of $8\lambda_c^3$ should have two holes. In a large finite realization of the configuration one can
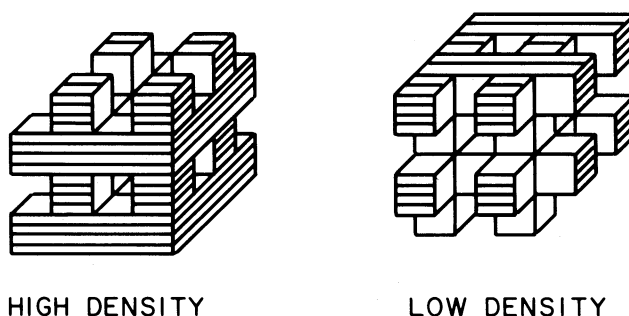
HIGH DENSITY

LOW DENSITY

Fig. 9.—Example of a sponge-like topology. Boundary surface has a negative curvature; it is the skew polyhedron with squares, six around a point.

see that if we leave all the tunnels connected on the plane $z = 0$, we can cut all the tunnels in the x and y directions everywhere else and still leave the surface connected. The unit cell contains tunnels in the x, y, and z directions, so the ability to make two cuts without disconnecting the surface means that three are on average two holes per unit cell.

We are now in a position to evaluate the average number of holes per unit volume in a distribution that has a cutoff in the power spectrum at wavelengths shorter than length λ_c and a Poisson spectrum at larger scales. Alternatively we can consider this as a spectrum with no cutoff but where λ_c is the scale over which we have smoothed the data. We can model such a spectrum as a series of cubical cells of length λ_c which are randomly assigned to the high- or low-density regions with 50% probability.

To determine the curvature of the boundary surface region we need to resolve ambiguities which arise when cubes meet at edges or corners. A cube touches 26 other cubes, it shares a face with six neighboring cubes, an edge with 12 neighboring cubes, and a vertex with eight cubes. Now four cubes meet at an edge, so if two of the four are to be neighbors, then the other two cannot be. Also, eight cubes meet at a vertex, and if two of them are neighbors, then the other three pairs cannot be. So a cube can have on average only 14 real neighbors: 6 with which it shares a face, $6 = 12/2$ with which it shares an edge, and $2 = 8/4$ with which it shares a corner. These ambiguities can be settled in a very concrete fashion if we offset or stagger the cubes slightly, as illustrated in Figures 10 and 11. By offsetting or staggering the cubes slightly we are avoiding the artificial degeneracy that brings eight cubes together at a vertex and returning to the generic situation encountered in a space-filling network where four polyhedrons meet at a vertex.

The offset configuration is illustrated in Figure 10. The squares drawn with solid lines illustrate the cubes on the first layer; the dashed squares illustrate the cubes on the second level. The cubes on the third level would be placed directly
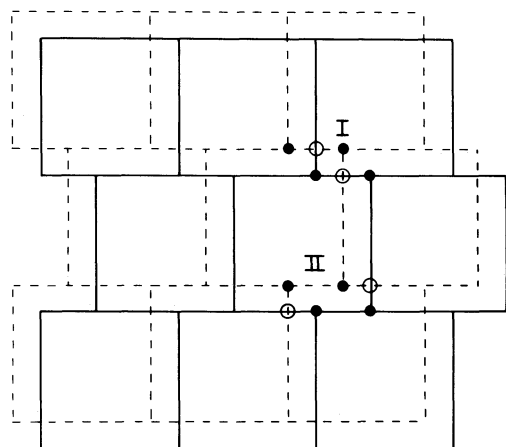
OFFSET CUBES

FIG. 10.—In analyzing topologies we divide space into a regular tesselation of unit cubes. To resolve ambiguities about which of the cubes meeting at a vertex are actually neighbors we may offset the cubes slightly. Squares drawn with solid lines represent the cubes on one level, and dashed squares represent the cubes on the next level. Each cube has 14 neighbors: six on its own level, four on the level above, and four on the level below. Vertices are of two types, I and II. Open circles represent minivertices of type A, and filled circles represent minivertices of type B.
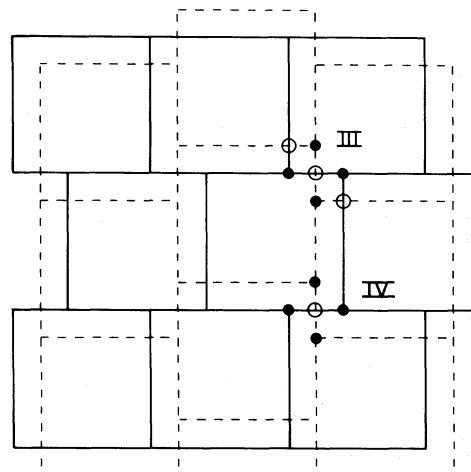
STAGGERED CUBES

FIG. 11.—Another tesselation of unit cubes may be constructed by staggering them slightly. Squares drawn with solid lines represent the cubes on one level, and the dashed squares represent the cubes on the next level. Each cube has 14 neighbors: six on its own level, four on the level above, and four on the level below. Vertices are of two types, III, and IV. Open circles represent minivertices of type A, and filled circles represent minivertices of type B.

above the corresponding cubes in the first level, and so forth. A vertex at which eight cubes originally met is replaced by six minivertices where four cubes meet. There are two equally frequent configurations labeled "I" and "II" on the diagram. Each vertex consists of two minivertices of type A (*open circles*) where two cubes from one level meet two cubes from the next level, and four minivertices of type B (*filled circles*) where one cube from one level meets three cubes from the next level.

Now we can calculate the average angle deficit produced at a minivertex A. Since there is a 50% chance for any cube to be high or low, there are 16 equally likely configurations for the four cubes. They give angle deficits as follows: $(H, H, H, H) = (L, L, L, L) = 0°$ (surface does not pass through the vertex); $(H, H, L, L) = (L, L, H, H) = (L, H, H, H) = (H, L, H, H) = (H, H, L, H) = (H, H, H, L) = (H, L, L, L) = (L, H, L, L) = (L, L, H, L) = (L, L, L, H) = 0°$; $(L, H, L, H) = (H, L, H, L) = (L, H, H, L) = (H, L, L, H) = -180°$. Thus the average angle deficit produced at a minivertex A is $D_A = -45° = -180° \times 4/16$.

For a minivertex B, four of the 16 cases produce angle deficits of $+90°$, four produce angle deficits of $-90°$, and eight produce angle deficits of $0°$, so the average angle deficit at a minivertex B is $D_B = 0°$. Thus a vertex of type I produces an average angle deficit of $D_I = 2D_A + 4D_B = -90°$. Now $D_{II} = D_I$, so the average vertex produces an angle deficit of $-90°$, and since there is one vertex per cube, the average value of I per volume of λ_c^3 is $-90° = -\pi/2$. Thus the mean number of holes per unit volume is

$$\frac{dg_s}{dV} = \frac{1}{8\lambda_c^3} . \qquad (6)$$

Note that we obtain the same results if we use the staggered cube configuration of Figure 11. In this case there are two types of vertices with average angle deficits $D_{III} = 3D_A + 4D_B = -135°$, $D_{IV} = D_A + 4D_B = -45°$. Since types III and IV occur with equal frequency, the average angle deficit per vertex is $-90°$, giving $dg_s/dV = 1/8\lambda_c^3$ just as in the offset

cube case. Note that in both the offset and staggered cases each cube, as expected, has 14 neighbors, six neighbors in its own layer, four neighbors from the layer below, four from the layer above. (Interestingly, the offset cube case is topologically equivalent to the space-filling tesselation of truncated octahedrons that forms a face centered cubic pattern; see Steinhaus 1969. Each truncated octahedron has 14 faces. Denoting every other one as high-density produces the sponge shown in Fig. 8 [hexagons, four around a point].)

The average area of boundary surface appearing per unit volume can be calculated as follows. Each cube has six faces and two cubes share a face, so there are three faces in the lattice for every cube. There is a 50% chance that any given face is a member of the boundary surface (occurring when one of the two cubes bordering it is high and the other low). Thus

$$\frac{dA}{dV} = \frac{3}{2\lambda_c}. \tag{7}$$

Finally the average curvature on the boundary surface is given by

$$\langle K \rangle = -\frac{\pi}{3\lambda_c^2}. \tag{8}$$

Thus we have shown that the boundary surface has an overall negative curvature and that it is multiply connected with many holes.

The high- and low-density regions are, with occasional exceptions, all connected. Every cube has 14 neighbors, so if one is sitting on a high-density cube, the probability that one is not connected to any other high-density cubes is $P = 2^{-14} = 6.1 \times 20^{-5}$. So it is possible to find some isolated clusters or voids, but they are extemely rare.

In Figures 12 and 13 we show that even with a resolution of $4 \times 4 \times 4$ and periodic boundary conditions it is possible to find configurations where the average curvature of the boundary surface is positive or zero. In Figure 12 is shown a positively curved boundary surface. One high-density cube is surrounded by 26 low-density cubes so as to be completely isolated. The boundary consists of the positively curved boundary surrounding this cluster and a spaghetti-type boundary surface with an average curvature of zero surrounding the low-density region. Thus the average curvature of the boundary surfaces is positive. In the repeating pattern both the high- and low-density regions are disconnected. Figure 13 shows a spaghetti-type topology where in the repeating structure high-density strands are surrounded by zero curvature boundary surfaces. In this model the high-density regions are
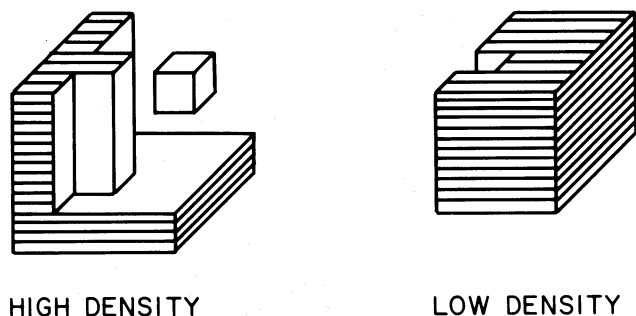

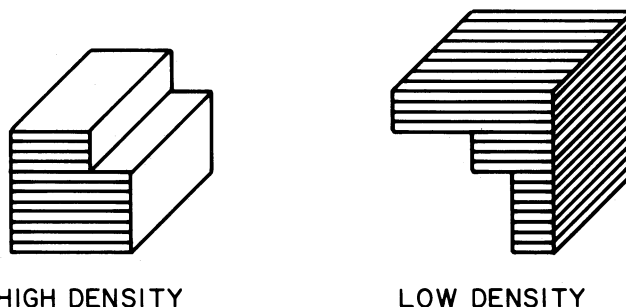HIGH DENSITY   LOW DENSITY

FIG. 13.—Example of a spaghetti-type topology in which the boundary has an overall average curvature of zero.

disconnected, but the low-density region is connected. Another topology that has boundary surfaces with zero curvature is a sandwich topology where the high- and low-density regions are alternating flat layers. We can construct one of these with a resolution of $4 \times 4 \times 4$ and periodic boundary conditions simply by making the first and third layers of cubes high density and the second and fourth layers low density. The boundary surfaces are parallel flat planes with zero curvature. The high- and low-density regions are equivalent. Both the high- and low-density regions are disconnected. The sandwich topology, like the sponge topology, treats the high- and low-density regions on an equal footing. It could result from a simple plane wave fluctuation in the initial conditions. (Sandwich topologies with wavy layers also have boundary surfaces with zero net curvature.) Of course, the sandwich topology must come from rather special initial conditions in which there are preferred directions and the fluctuations are in phase. The point of these examples is that although there are configurations with positive or zero curvature, there are not very many of them, and with random phases in the initial conditions configurations with negative curvature are much more likely, in fact, the average value of the curvature is negative.

The results have been derived for a Poisson spectrum $n = 0$. This is a reasonable approximation to CDM scenarios whose index changes from $n = -3$ at very small scales to $n = +1$ at very large scales and whose index is near $n = 0$ on the scales of interest. We have already seen that neutrino models with $n = +1$ at scales larger than the cutoff still show holes and a sponge-like topology. It is interesting to show why an $n = -1$ spectrum with anticorrelations at large scales will still theoretically produce a sponge-like topology. One way to produce an $n > 0$ anticorrelated spectrum is to place the galaxies approximately on the vertices a regular lattice rather than in a Poisson distribution (see Gott 1979). This assures that the fluctuations on large scales are less than in a Poisson distribution and therefore gives a spectrum with $n > 0$. Being nearly on the vertices of a regular lattice, the galaxies are anticorrelated at small scales since they are not allowed to have near neighbors. We can duplicate this type of distribution by placing high- and low-density cubes of size λ_c in a regular three-dimensional checkerboard pattern such that the high-density cubes form a face centered cubic lattice. If you sit on a high-density cube, you have six nearest neighbors (at a center-to-center distance of λ_c) which are all low, thus giving anticorrelation at this scale. The next 12 nearest cubes (at a distance of $\sqrt{2}\lambda_c$) are all high, but then the next eight (at a distance of $\sqrt{3}\lambda_c$) are low. In the staggered or offset cube configuration, of the high-density cube's 14 actual neighors, eight are low and only six are high.

HIGH DENSITY   LOW DENSITY

FIG. 12.—Example where the topology includes an isolated high-density cluster. The boundary has an overall average curvature which is positive.

Putting the high- and low-density cubes in a face-centered cubic three-dimensional checkerboard pattern simulates an anticorrelated $n > 0$ spectrum. The mean angle deficit per vertex in this configuration averaged over the staggered and offset cases is $D = -270°$, giving an average density of holes $dg_s/dV = 3/8\lambda_c^3$. So this type of distribution leads to a sponge-like topology as well.

The simplest way to determine g_s from a pair of figures such as Figures 2a and 2b is to consider the high-density region to be a finite block of driftwood bounded by not only the boundary surface but by the intersections of the high-density region with the faces of the cubical repeat cell just as it appears in Figure 2a. Then we can define g_H^* as the genus of the high-density region, the number of complete cuts we can make in the high-density block of driftwood without cutting it into two pieces. Similarly, g_L^* is the genus of the low-density region, the number of cuts we can make in the finite low-density region portrayed without cutting it into two pieces. Let V_E be the number of edge vertices, that is the number of points where the boundary surface intersects an edge of the cubical repeat cell. Then one can show that

$$g_s = \frac{-1}{4\pi} \int K dA = \frac{1}{2}\left(g_H^* + g_L^* + \frac{V_E}{4} - 1\right). \quad (9)$$

Even with structures as simple as those shown in Figures 1 and 2, it is surprisingly difficult to determine g_s by hand using this method, having only two-dimensional drawings like Figures 1 and 2 to consult. Even using two or more views of the cube from different directions it is hard to determine g_H^* and g_L^* because some of the structure can still remain hidden from view. Using available views and equation (9), we judge that $g_s = 3$ for the CfA sample (Fig. 1). For the CfA sample $\lambda_c \sim 0.33L$, and in the volume L^3 using equation (6) we expect to find approximately three holes. Similarly we judge that $g_s = 5$ for the neutrino initial conditions (Fig. 2). In this model $\lambda_c = 0.36L$ and using equation (6) we expect approximately three holes. We judge that $g_s = 2$ for the surface in Figure 6, again in accord with expectations. For structures any more complicated than these a computer algorithm would certainly be desirable.

We may ask what happens to the boundary between the high- and low-density regions with a Poisson spectrum if we were to not take the median density as the dividing line, but say the upper quartile instead. Let X be the fraction of the volume occupied by the high-density region. Then the average angle deficit at a minivertex A is $D_A = -4\pi X^2(1 - X)^2$, and at a minivertex B is $D_B = \pi[X^3(1 - X) + X(1 - X)^3] - 2\pi X^2(1 - X)^2$. Each vertex has on average $D = 2D_A + 4D_B$, so

$$D = 4\pi[X^3(1 - X) + X(1 - X)^3 - 4X^2(1 - X)^2]. \quad (10)$$

The mean number of holes per unit volume is

$$\frac{dg_s}{dV} = \frac{4X^2(1 - X)^2 - [X^3(1 - X) + X(1 - X)^3]}{\lambda_c^3}, \quad (11)$$

and

$$\frac{dA}{dV} = \frac{6X(1 - X)}{\lambda_c}, \quad (12)$$

$$\langle K \rangle = \frac{4\pi(1/6 - X + X^2)}{\lambda_c^2}. \quad (13)$$

Now for $X = 0.5$, $\langle K \rangle = -\pi/3\lambda_c^2$, as we obtained earlier. In fact, $\langle K \rangle$ reaches a minimum at $X = 0.5$. The mean value of the curvature $\langle K \rangle$ approaches a maximum of $2\pi/3\lambda_c^2$ as either $X \to 0$ or $X \to 1$. In these cases we have either isolated clusters of size λ_c as $X \to 0$ or isolated voids of size λ_c as $X \to 1$. Now $\langle K \rangle = 0$ for $X = 0.5 \pm (6)^{-1/2}$. Thus if we want to obtain isolated clusters of spherical topology (white polka dots on a black background), we must set $X < 0.5 - (6)^{-1/2} = 0.211$. When we reach the critical point $X = 0.211$ where the mean curvature of the boundary surface is zero, this does not mean that we have the spaghetti topology. Instead, it is likely that we will get a sponge with many holes plus some isolated clusters. When the number of holes is equal to the number of separate pieces, the overall genus of the surface is zero and the average curvature is zero. If we want to obtain isolated voids of spherical topology, we must set $X > 0.5 + (6)^{-1/2} = 0.789$. By comparison Shandarin and Zeldovich (1983) have noted in passing that in the case of a pure, random, but smooth function f percolation emerges in the phase where $f > f_c$ occupies more than 16% of the total volume. Thus percolation occurs in both the high- and low-density phases, provided $16\% < X < 84\%$ using our notation. (Despite this they argued that the voids would be isolated because they found that only 8% of the matter was expanding faster than the universe in all three directions, and this they wished to associate with void material. By contrast, we would note that their results are consistent with a sponge-like topology with a median density contour in the initial conditions, and we would note that this remains virtually unchanged up to the present epoch.) Note that percolation and connectedness are not the same thing. In the spaghetti topology, both the high- and low-density regions percolate, but only the low-density region is connected. If we want to maximize the number of clusters of spherical topology found, we must maximize D. This occurs at $X = 0.0918$ where $D = 0.04167$. Thus at this value of X we obtain the highest possible density of isolated spherical topology clusters $\rho_{CL} = 1/24.0\lambda_c^3$. This result with a Poisson distribution is a factor of ~ 3 lower than the absolute maximum density of clusters that it would be possible to have if one arranged them on a lattice with $X = \frac{1}{8}$ and a cluster as one unit cube in a repeat pattern that was $2 \times 2 \times 2$ unit cubes in size. This would give $\rho_{CL} = 1/8\lambda_c^3$.

The division of space into cubes provides the basis for constructing a computer algorithm for measuring the genus of the boundary surface of a given configuration. For more complicated sponge-like topologies like that in Figure 4 a computer algorithm to measure the topology is really needed. Suppose we have a smoothed density function $\rho(x, y, z)$ and a critical density ρ_c used to divide the high- and low-density regions. Pick a grid size such that the size of a unit cell is smaller than the smoothing length and smaller than any likely holes or clusters one wants to measure. Then construct the density matrix $\rho(i, j, k)$ showing the value of the density at the center of each cell. If $\rho(i, j, k) \geq \rho_c$, set $\rho(i, j, k) = 1$; otherwise, set $\rho(i, j, k) = 0$. Let the vertex at the upper left back corner of cell (i, j, k) be labeled vertex (i, j, k). The angle deficit at this vertex $D(i, j, k)$ depends on the values of the density in the eight surrounding cells, $\rho(i + m, j + n, k + o)$ where $m, n, o = 0$ or 1. Each of the 256 possible configurations can be identified by an eight-bit binary number, and the value of $D(i, j, k)$ can be found from a previously calculated look-up table. The look-up table is calculated using either a staggered or offset cube configuration using the minivertices. Each vertex must be identified by type (I, II,

III, IV) and whether the dotted or solid cubes (in Figs. 10 and 11) are on the top level. Depending on its position each vertex will use one of eight look-up tables. Most vertices will not be on the boundary, so the first thing will be to check if all eight surrounding cell neighbors are either high or low. If this is the case, $D(i, j, k) = 0$ and no further calculations are necessary. Periodic boundary conditions can be treated in the usual way. The genus of the surface will be given by

$$g_s = - \sum_{i,j,k} D(i, j, k)/4\pi .$$

If we want to find out of how many separate pieces the high-density region consists, we can use standard "a friend-of-a-friend is a friend" algorithms to make a group calalog of all high-density cells that are neighbors. Such antomated methods should be invaluable in analyzing the topology in complicated situations.

IV. CONCLUSIIONS AND AREAS FOR FURTHER RESEARCH

In this paper we have studied the relative connectedness of the high- and low-density regions in the universe using a median density contour which divides space into two equal volumes. We find that the CfA data show a sponge-like topology where the high- and low-density regions are each connected. Both are interlocking and equivalent. One might say that there is just one connected supercluster and one connected void. The sponge-like topology arises naturally from the initial conditions in inflationary models where the fluctuations are due to quantum noise. In the initial conditions the connectedness of the high- and low-density regions must be identical because a change of sign in the random quantum fluctuations would reverse their roles. In adiabatic or massive neutrino models where there is a short-wavelength cutoff λ_c and random phases on larger scales, this leads to a sponge-like topology with hole sizes of order λ_c. While the fluctuations are still growing in the linear regime there is no change in topology, and at the scales of interest we are just coming out of the linear regime today, so the topology remains sponge-like at the present epoch. Since galaxy data consist of a series of δ-functions, the data must be smoothed by at least the mean intergalaxy distance scale before meaningful density contour maps can be made. Smoothing by convolution with a Gaussian is equivalent to multiplying the Fourier power spectrum by a Gaussian and damps the small-scale fluctuations in exactly the same way Landau or Silk damping would do. This introduces a short-wavelength cutoff λ_c equal to the smoothing diameter. Thus CDM scenarios also show a sponge-like topology with a hole size of order λ_c. The CfA data show a sponge-like pattern that is consistent with this. A heavy neutrino model with a Landau damping scale $\lambda_c \approx 10h^{-1}$ Mpc also gives a sponge-like topology that fits the data well. Some theories of galaxy formation like the Ostriker, Cowie, and Ikeichi model really produce a cell structure topology initially, but nonlinear gravitational instability effects can rip holes in the cell walls and can convert it into a sponge-like topology. In such scenarios the high- and low-density regions are not required to be equivalent. It is hard to say what topology would be produced by string-assisted galaxy formation, but if the galaxy clustering has a topology that mimics that of the strings themselves, then it is a spaghetti-type topology.

We have shown that an important technique in analyzing the topology of the high- and low-density regions is studying the curvature of the boundary surface that separates them. We find that the surface has an overall negative curvature, and via the Gauss-Bonnet theorem we are led to the conclusion that it has many holes. A distribution with an $n = 0$ initial density fluctuation spectrum and short-wavelength cutoff of λ_c has a mean volume density of holes of $dg_s/dV = 1/8\lambda_c^3$. Such studies are facilitated by approximating the boundary surface with a polygon network where the curvature is confined to the vertices. This technique makes it possible to develop automated computer algorithms for measuring the topology directly.

The sponge-like topology explains a number of things in the observed distribution of galaxies. It explains how the universe can have a frothy appearance without being divided neatly into cells. It creates a messy appearance with clusters being connected and voids spilling lazily into each other.

There are anumber of interesting areas for future research. Certainly it would be interesting to look at the topology as a function of density contour. If the contour is set at the median value, we should get a sponge-like topology. If the density contour is set high enough, we should see isolated clusters. It would be interesting to plot the genus of the boundary surface as a function of the fraction of the volume X in the high-density phase. We have produced such a formula $g(X)$ for $n = 0$ initial conditions with a short-wavelength cutoff. It would be interesting to see such a curve for observed data sets and simulations where nonlinear effects in the clustering could be observed. At the highest density enhancements this constitutes a study of the multiplicity function of rich clusters (see Gott and Turner 1979). This gives us a way to bring a quantitative analysis to the study of the topology of large-scale structure in the universe. In one case we have looked at the topology of a higher density contour of the final conditions of the massive neutrino model shown in Fig. 3. We find, for example, a dense, thin filament running down the center of what was a high-density tunnel in the initial conditions. The sponge-like topology provides many columns and holes out of which it is natural to form one-dimensional filaments. This may explain why a number of simulations using massive neutrinos (where the density contour was chosen above the median) show one-dimensional filaments rather than two-dimensional sheets (Melott 1985; Frenk, White and Davis 1983). More investigation of the relationship between the original sponge-like topology and the higher density contours related to it would be useful.

It would be interesting to look further at CDM models. The one we did showed a sponge-like topology with the smallest holes equal to the size of the smoothing length, as expected. However, the largest features such as lengths of tunnels were perhaps related to the scale at which the spectrum index n becomes positive. This type of sponge might theoretically be expected to show two scales. CDM models with biased galaxy formation might also be interesting to study (see Melott and Fry 1985). One nice thing about our method is that it should be rather insensitive to biased galaxy formation. In biased galaxy formation models M/L is expected to be a monotonic function of density, so that contours of constant luminosity density should also be contours of constant density. The median density contour and the median luminosity density contour (defined as the contour which divides the volume into two equal parts) should in principle, be identical. However, if the biased galaxy formation produces a step function in M/L versus density, this could create some statistical problems in measurement.

On the observational side the most important thing is to

explore the connectedness of the low-density regions. It would be useful to have a test for evaluating whether the low-density regions are connected that, like the Shandarin percolation test, could be applied directly to the galaxy data and was not tied directly to measuring density contours as we have done. An investigation of whether the famous great voids are truely isolated would be quite interesting. Are they really surrounded on all sides by high-density regions? In this regard it is interesting to note that while the Kirshner *et al.* void in Bootes appears to have very well defined front and back edges, it appears to continue on in at least one direction perpendicular to the line of sight. Deep three-dimensional redshift surveys are needed. This is time consuming but necessary work. One- or two-dimensional surveys simply do not give us the information we need. A two-dimensional slice through a universe with a Swiss cheese topology can look the same as a two-dimensional slice through a universe with a sponge-like topology, for example. Both can show holes. The crucial question is whether the voids are completely isolated or whether they are connected to each other by low-density tunnels in three dimensions. We really need full three-dimensional information to answer this question. In looking at observational samples it is important to remember that many of the most striking features such as collapsed clusters or thin filaments or sheets are produced by nonlinear gravitational effects. For example, a high-density, reasonably thick bridge present in the initial conditions can collapse to a very thin, high-density filament by the present epoch. This is seen in *N*-body simulations. While nonlinear effects can produce very high density contrast features which are spectacular, they do not tell us very much about the initial conditions. If we want to find out about the initial conditions, we should start with a deep three-dimensional survey. Then we should smooth the data with a smoothing length which exceeds the correlation length. This way we will be looking at fluctuations which are only just now beginning to come out of the linear regime. Then we should construct the median density contour and measure its topology. If the structure has been formed by gravitational instability from initial quantum

fluctuations, then we expect to find that the median density contour gives a sponge-like topology. As we have argued, if we pick instead a high enough density contour, we will find isolated clusters, and if we pick a low enough density contour we will find isolated voids (see Centrella and Melott 1983). The important feature is that the high- and low-density regions are treated equally. We expect to find as many clusters as voids, and we expect as many bridges connecting clusters as low-density tunnels connecting voids.

It is hoped that this program of observational and theoretical work will lead to a more quantitative analysis of the topology of the large scale structure of the universe and its relation to the topology in the initial conditions.

Note added in manuscript—Since submitting this paper we have made some further progress which will be reported in future papers. Hamilton, Gott, and Weinberg (1986) have derived a general formula for the number of holes per unit volume in the initial conditions for a general power spectrum of Gaussian fluctuations with random phases. Bardeen *et al* (1986) have independently derived the same formula for different purposes using a completely different method. The topology of the median contour is sponge-like, independent of the form of the power spectrum, and the qualitative features of equation (11) are retained. Einasto *et al.* (1986) have used the methods described in this paper to study three redshift samples from the CfA data set, the largest containing 526 galaxies. They constructed median density contours and studied the topology with varying resolution. They found that the topology was sponge-like, confirming the results presented here.

REFERENCES

Aarseth, S. J., Gott, J. R., and Turner, E. L. 1979. *Ap. J.*, **228**, 664.
Bahcall, N., and Soniera, R. M. 1983, *Ap. J.*, **270**, 20.
Bardeen, J. M., Bond, J. R., Kaiser, N., and Szalay, A. S. 1986, preprint.
Blumenthal, G. R., Faber, S. M., Primack, J. R., and Rees, M. J., 1984, *Nature*, **311**, 517.
Bond, J. R., Efstathiou, G., and Silk, J. 1980. *Phys. Rev. Letters*, **45**, 1980.
Centrella, J., and Melott, A. 1983, *Nature*, **305**, 196.
Coxeter, H. S. M. 1937, *Proc. London Math Soc.*, **43**, 33–62.
Davis, M., Efstathiou, G., Frenk, C., and White, S. 1985, *Ap. J.*, **292**, 371.
Doroshkevich, A. G., Sunyaev, R. A., and Zeldovich, Ya. B. 1974, in *IAU Symposium 63 Confrontation of Cosmological Theories with Observational Data*, ed. M. S. Longair (Dordrecht: Reidel), p. 213.
Doroshkevich, A. G., Zeldovich, Ya. B., Sunyaev, R. A., and Khlofov, M. Yu. 1980, *Soviet Astr. Letters*, **6**, 252.
Einasto, J., Klypin, A. A., Saar, E., and Shandarin, S. F. 1984, *M.N.R.A.S.*, **206**, 529.
Einasto, J., Einasto, U., Melott, A., and Saar, E. 1966, in preparation.
Einasto, J., Klypin, A. A., and Shandarin, S. F. 1983, in *IAU Symposium 104, Early Evolution of the Universe and Its Present Structure*, ed. G. O. Abell and G. Chincarni (Dordrecht: Reidel), p. 405.
Einasto, J., Miller, R. H. 1983, in *IAU Symposium 104, Early Evolution of the Universe and Its Present Structure*, ed. G. O. Abell and G. Chincarini (Dordrecht: Reidel), p. 405.
Frenk, C. S., White, S. O. M., and Davis, M. 1983, *Ap. J.*, **271**, 417.
Gott, J. R. 1967, *Am. Math. Month.*, **74**, 497.
———.1979, in *Les Houches XXXII, Physical Cosmology*, ed. R. Balian, J. Audouze, and D. N. Schramm, (Amsterdam: North Holland), p. 561.
———.1982, *Nature*, **295**, 304.
———. 1985, *Ap. J.*, **288**, 422.
Gott, J. R., and Dickinson, M. 1986, in preparation.
Gott, J. R., and Turner, E. L. 1979, *Ap. J.*, **234**, 13.

Gott, J. R., and Statler, T. S. 1984, *Phys. Letters*, **136B**, 157.
Hamilton, A. J. S., Gott, J. R., and Weinberg, D. 1986, *Ap. J.*, submitted.
Heavens, A. 1985, *M.N.R.A.S.*, **213**, 143.
Hogan, C. J. 1984, *Ap. J. (Letters)*, **284**, L1.
Hogan, C. J., and Rees, M. J. 1984, *Nature*, **311**, 109.
Ikeuchi, S. 1981, *Pubs. Astr. Soc, Japan*, **33**, 221.
Joeveer, M., and Einasto, U. 1978, in *IAU Symposium 79, The Large Scale Structure of the Universe*, ed. M. S. Longair and J. Einasto (Dordrecht: Reidel), p. 241.
Kaiser, N., and Stebbins, A. 1984, *Nature*, **310**, 391.
Kirshner, R. P., Oemler, A., and Schechter, P. L. 1979, *A.J.*, **84**, 951.
Kirshner, R. P., Oemler, A., Schechter, P. L., and Schectman, S. A. 1981, *Ap. J. (Letters)*, **248**, L57.
Klypin, A. A., and Shandarin, S. F. 1983, *M.N.R.A.S.*, **204**, 89.
Mandelbrot, B. B. 1983, *The Fractal Geometry of Nature* (San Francisco: Freeman).
Matsuda, T., and Shima, E. 1983, Kyoto University preprint.
Melott, A. 1983, *M.N.R.A.S.*, **202**, 595.
———. 1985, *Ap. J.*, **289**, 2.
Melott, A., Einasto, J., Saar, E., Suisclu, I., Klypin, A., and Shandarin, S. 1983, *Phys. Rev. Letters*, **51**, 935.
Melott, A., and Fry, J. N., 1986, *Ap. J.*, **305**, 1.
Ostriker, J. P., and Cowie, L. L. 1981, *Ap. J. (Letters)*, **243**, L127.
Peebles, P. J. E. 1980, in *The Large Scale Structure of the Universe* (Princeton: Princeton University Press).
———. 1982, *Ap. J. (Letters)*, **263**, L1.
Schramm, D. N. 1985, unpublished.
Shandarin, S. F. 1983, *Pis'ma Astr. Zh.*, **9**, 195.
Shandarin, S. F., and Zeldovich, Ya. B. 1983, *Comments Ap.*, **10**, 33.
Schwarzschild, M. 1980, private communication.
Soneira, R. M., and Peebles, P. J. E. 1978, *A.J.*, **83**, 845.

Steinhaus, H. 1969, *Mathematical Snapshots* (New York: Oxford University Press).
Szalay, A. S., and Bond, J. R. 1983, *IAU Symposium 104, Early Evolution of the Universe and Its Present Structure*, ed. H. O. Abell and H. Chincarini (Dordrecht: Reidel), p. 307.
Turner, E. L., and Gott, J. R. 1976. *Ap. J.*, **209**, 6.
Vilenkin, A. 1981*a*, *Phys. Rev. Letters*, **46**, 1169.
———. 1981*b*, *Phys. Rev. D.*, **23**, 852.

Vishniac, E. T., and Ostriker, J. P. 1984, Princeton Observatory preprint No. 130.
Wells, A. F. 1969, *Acta. Crystallogr.*, **B25**, 1711.
———. 1977, *Three Dimensional Nets and Polyhedra* (New York: Wiley).
White, S., Frenk, C., and Davis, M. 1983, *Ap. J.* (*Letters*), **274**, L1.
Zeldovich, Ya. B. 1978, in *IAU Symposium 79, The Large Scale Structure of the Universe*, ed. M. S. Longair and J. Einasto (Dordrecht: Reidel), p, 409.
———. 1980, *M.N.R.A.S.*, **192**, 663.

M. Dickinson: Department of Astronomy, University of California, Berkeley, CA   94720

J. R. Gott: Department of Astrophysical Sciences, Princeton University, Princeton, NJ   08544

A. Melott: Astronomy and Astrophysics Center, University of Chicago, 6540 S. Ellis Ave., Chicago, IL   60637